

UNCLASSIFIED

*This Document
Reproduced From
Best Available Copy*

AD **431918**

DEFENSE DOCUMENTATION CENTER

FOR

SCIENTIFIC AND TECHNICAL INFORMATION

CAMERON STATION, ALEXANDRIA, VIRGINIA



UNCLASSIFIED

REPRODUCTION QUALITY NOTICE

This document is the best quality available. The copy furnished to DTIC contained pages that may have the following quality problems:

- **Pages smaller or larger than normal.**
- **Pages with background color or light colored printing.**
- **Pages with small type or poor printing; and or**
- **Pages with continuous tone material or color photographs.**

Due to various output media available these conditions may or may not cause poor legibility in the microfiche or hardcopy output you receive.



If this block is checked, the copy furnished to DTIC contained pages with color printing, that when reproduced in Black and White, may change detail of the original copy.

NOTICE: When government or other drawings, specifications or other data are used for any purpose other than in connection with a definitely related government procurement operation, the U. S. Government thereby incurs no responsibility, nor any obligation whatsoever; and the fact that the Government may have formulated, furnished, or in any way supplied the said drawings, specifications, or other data is not to be regarded by implication or otherwise as in any manner licensing the holder or any other person or corporation, or conveying any rights or permission to manufacture, use or sell any patented invention that may in any way be related thereto.

AD No. 431918



FILE COPY

⑤ 150 700 64-10
EXPLOSIVES RESEARCH CENTER

HYPERVERLOCITY IMPACT PHENOMENA

Quarterly Report

September 1, 1963 to November 30, 1963

BUREAU OF MINES, PITTSBURGH, PA.

MAR 15 1964

30 P #2.60
UNITED STATES
DEPARTMENT OF
THE INTERIOR

(5) 150-704

(6)

HYPERVERLOCITY IMPACT PHENOMENA

(7)

Quarterly Report.

September 1, 1963 to November 30, 1963

Prepared for:

U. S. Army Ordnance
Ballistic Research Laboratory
Aberdeen Proving Ground, Maryland
Approved Proposal No. 3175
Authorization No. 4086

(10) by

Richard W. Watson,
Karl R. Becker,
Frank C. Gibson,

Approved by:

Robert W. Van Dolah
Robert W. Van Dolah
Research Director
Explosives Research Center

U. S. Department of the Interior
Bureau of Mines
Pittsburgh, Pa.
February 5, 1964

(11)

HYPERVERELOCITY IMPACT PHENOMENA

Introduction

This report on Hypervelocity Impact Phenomena consists of two sections describing methods and analyses of behind target effects in three metals and the development and performance of two new explosive projector systems that are to be applied to subsequent investigations of hypervelocity impact.

Shock Wave Studies in Three Metals

In a recent paper summarizing hypervelocity impact work carried out at this Center^{1/}, it was concluded that a measure of the peak shock wave pressure incident on the back surface of impacted targets would permit a quantitative interpretation of many behind target effects. As a logical extension of the earlier work, several phases of an experimental program aimed at a quantitative description of behind target effects in terms of the shock pressure generated by high velocity impacts have been undertaken. These studies have also involved shock waves generated by detonating explosives.

Experimental Techniques

While many techniques have been used to determine the pressures associated with shock waves in solids, one of the simplest is the plate-pellet method which is an application of the Hopkinson principle that has been extensively described elsewhere^{2/}. Briefly,

^{1/} Watson, R. W., K. R. Becker, and F. C. Gibson. Thin Plate Perforation Studies with Projectiles in the Velocity Range from 2 to 5 km/sec. Sixth Symposium on Hypervelocity Impact, Cleveland, Ohio, April 30 - May 2, 1963.

^{2/} See for example Rinehart, J. S. and J. Pearson. Behavior of Metals Under Impulsive Loads. Published by the American Society for Metals, 1954.

a pellet of like material is attached to the free surface of the material that is to undergo shock loading. The pellet serves to absorb a certain portion of the momentum associated with the incident wave; the amount of momentum attained by the pellet depends on the thickness of the pellet relative to the length of the pressure pulse. In principle, it is possible to map out the entire pressure pulse profile by varying the pellet thickness over a suitable range. In the experiments described here the pellet is purposely kept thin and its average velocity is taken as representative of the initial free surface velocity of the shock-loaded specimen. While there are objections that could be raised concerning the validity of this assumption, a comparison between the results of free surface velocities obtained by pin technique and free surface velocity estimates obtained by the pellet method shows that the latter method gives results that are precise enough for present requirements. The experimental arrangements used to obtain the two data sets are illustrated in figures 1 and 2.

In figure 1, the shock wave is generated by a detonating tetryl charge having a diameter of 1.0 in and a length of 1.0 in; the initial density of the tetryl was 1.57 gm/cm^3 . A distance-time record of the initial motion of the free surface of the metal attenuator was provided by recording the pulses generated by the progressive shorting of four pins when contacted by the grounded attenuator plate. The pins were pointed 2-56 brass machine screws and were held in position by means of a Lucite block. The pins were equally spaced on a circle of 1/2-in diameter and were positioned 0.001, 0.011, 0.021, and 0.031 inch from the free surface of the metal attenuator. Close spacing was chosen to eliminate the effects of subsequent acceleration of the plate due to multiple shock reflections.

Figure 1 also shows two channels of a multi-channel pulse-

forming network that produces pulses having a duration of about 0.1 μ sec and an amplitude of approximately 10 volts when the negative side of the 100 pf capacitor is shorted to ground.

Figure 2 illustrates the experimental arrangement used to determine the time of flight of a pellet over a fixed distance. In this case, a high-speed oscilloscope is triggered when the ionized detonation products electrically short a twisted pair of #28 enameled copper wires placed on the periphery of the charge. The time-of-arrival of the pellet is observed when the pellet shorts a similar switch placed a fixed distance from the free surface of the metal attenuator. This second switch is connected to an R-C circuit that produces a pulse that is fed into the y-axis amplifier of an oscilloscope. The average pellet velocity is then calculated with corrections made for the time required for the detonation wave to pass from the initiation switch to the attenuator plate and for the shock wave to traverse the plate. An initiation delay, correction of approximately 0.2 μ sec, is also made.

Figure 3 is a typical oscillogram showing a series of four pulses obtained in a trial using a 1/8-in thick brass attenuator plate; a pellet velocity record obtained with a similar attenuator plate is also presented.

Distance-time measurements obtained by means of the pin technique are presented in table 1 for 1/4-in thick 2024-T3 aluminum attenuators and 1/8-in thick brass attenuator plates; five trials were carried out in each case. As indicated in figure 4, the slope of straight lines fitted through the average of five trials gave velocities of 1.68 mm/ μ sec for the aluminum attenuator and 1.02 mm/ μ sec for the brass attenuator.

Six pellet velocity measurements were made with the 1/4-in

aluminum attenuator. The individual values were 1.66, 1.62, 1.66, 1.58, 1.56, and 1.59 mm/ μ sec, representing an average velocity of 1.61 mm/ μ sec. Five trials carried out with the 1/8-in brass attenuators gave values of 1.01, 1.06, 1.05, 1.06, and 1.02 mm/ μ sec with an average of 1.04 mm/ μ sec.

As can be seen, the results of the two experimental techniques compare favorably. In both cases, the pellet technique gave results that were lower than those obtained by the pin technique; for the case of the 1/4-in aluminum attenuator, the discrepancy amounted to about 4 percent while, for the brass attenuator, the difference was roughly 2 percent. These differences probably can be attributed to air-drag effects which could be considered if more precise results were required.

Experimental Results with Aluminum, Magnesium, and Steel

In view of the accuracy and simplicity of the pellet technique, it was used in an investigation of shock wave attenuation and characteristic target damage using explosive-generated shock waves. Three target materials used were: aluminum, designated Al-2024-T3; magnesium, designated AZ-31B-H24; and a steel alloy, designated N-4130, S-18729. These materials were supplied by the Firestone Tire and Rubber Co., Defense Research Division, Akron, Ohio. In these experiments, pellet velocity was measured as a function of plate thickness using an explosive load consisting of a 1-in diameter x 1-in long tetryl charge having an initial density of 1.57 gm/cm³. The tetryl charge was initiated with Primacord. Target thickness was varied for each of the three materials to cover target damage effects ranging from perforation through back surface spalling to slight bulging.

The results of this series of experiments are presented in

tables 2, 3, and 4 in terms of wafer velocity as a function of target thickness. The target damage observed in each case is also given. Independent tests carried out with similar target arrangements with omission of the wafer produced identical damage effects. Calculated values of the incident shock pressure associated with the free-surface velocity estimates obtained from the pellet velocities are also given in tables 2, 3, and 4. The Hugoniot data for aluminum and magnesium were taken from Rice, McQueen, and Walsh^{3/}. For the case of the steel targets, the pressures associated with the free-surface velocity estimates were calculated for a linearized equation of state of the form $U_s = 4.632 + 1.385 u_p^{4/5}$. This is admittedly somewhat arbitrary. However, inasmuch as the multiple shock structure in iron casts considerable doubt on the validity of free surface velocity-pellet equivalence assumption, this choice is as reasonable as any other. From these data, approximate critical thickness for spallation under these conditions can be estimated for the three materials. The critical spallation thickness is defined as that target thickness which will barely spall subsequent to the reflection of the incident pressure wave. The corresponding incident pressure then can be interpreted as the peak stress necessary to produce a single spall. These values are summarized in table 5 for the three target materials tested. The value for aluminum agrees well with the value reported by Erkman^{5/}. The value for steel is in the

3/ Rice, M. H., R. G. McQueen, and J. M. Walsh. Solid State Physics, v 6, Academic Press Inc., 1958.

4/ Taylor, John W., and Melvin H. Rice. Elastic-Plastic Properties of Iron. J. Appl. Phys, v 34, No. 2, February 1963.

5/ Erkman, J. O. Decay of Explosively Induced Shock Waves in Solids and Spalling of Aluminum, Poulter Laboratories Technical Report 008-60, Stanford Research Institute, Menlo Park, California, August 10, 1960.

range given by Nahmani^{6/}. Comparison data for magnesium were not available. The values for aluminum and steel are considerably in excess of the values reported by Rinehart^{7/}. While there is some question as to the usefulness of these numbers from a mechanistic point of view, it is felt that they will be of practical value in the investigation of later hypervelocity impact experiments to be conducted with these same target materials.

Hypervelocity Projector Development

Two new explosive projector systems that are scaled versions of systems developed at the Ballistic Research Laboratories, Aberdeen Proving Ground, Md., are now available for hypervelocity impact studies. One is a one-half linear scale size of an inhibited jet-type projector system described in a previous report^{8/}. It produces an aluminum projectile of about 0.37 gram mass and a velocity of about 9.3 km/sec. The other system is a double linear scale size of an air-cavity type projector and produces a steel projectile of about 1.5 grams mass and a velocity of about 4.7 km/sec. Although the masses and velocities of the two projectiles are considerably different, the kinetic energies are nearly the same.

The One-Half Scale Inhibited Jet Projector

A drawing of the one-half scale inhibited jet projector is shown in figure 5; it is essentially a shaped charge containing a

^{6/} Nahmani, G. Experimental Investigation of Scabbing Produced in Mild Steel Plates by Plane Stress Waves. *Les Ondes de Detonation* (International Colloquium on Detonation Waves). Editions du Centre National de la Recherche Scientifique, Paris, 1962 (pp. 451-8).

^{7/} See work cited in reference 2.

^{8/} Watson, R. W., K. R. Becker, J. E. Hay, and F. C. Gibson. Hypervelocity Impact Phenomena. Bureau of Mines Quarterly Report, U. S. Army Ordnance, Aberdeen Proving Ground, Md., June 1, 1963 to August 31, 1963.

conical aluminum liner. Normally, the collapse of the liner produces a rather long jet having a velocity gradient along its length; however, a short coherent projectile is formed by the use of a Lucite plug (inhibitor) to prevent the collapse of the base elements of the liner. The details of the conical liner and inhibitor configuration were based upon the Scale I inhibited jet projector developed by the Ballistic Research Laboratories. Initial tests showed that certain modifications of the Scale I geometry were necessary to improve projector performance.

With a given cone design, the performance of the projector may be influenced by (1) changing the height of the Lucite inhibitor and (2) changing the height of the column of explosive extending above the spit-back tube. A projector producing a single projectile having a length to diameter ratio of about three, at impact, was desired. Radiographs were taken of all projectiles to evaluate their acceptability.

The effect of inhibitor height on projectile formation is illustrated in figure 6. Radiographs are shown for inhibitor heights of (a) 5/8 in, (b) 3/4 in, and (c) 1 inch. The head of composition B explosive was constant and extended 5/8 in above the top of the spit-back tube. A 1-5/8 in diameter x 1/2-in long tetryl booster was used for these trials. The figure demonstrates that the amount of projectile material decreases as inhibitor height increases. The projectiles in this sequence of photographs have traveled a distance of about 24 inches. With a 5/8-inch high inhibitor (figure 6(a)), a rather long segmented projectile was formed. With a 3/4-in high inhibitor (figure 6(b)), the projectile has been considerably shortened; and in figure 6(c), the one-inch inhibitor prevents the formation of any high velocity projectile material. In the first two photographs, the velocity of projectile

material was about 9.4 km/sec.

On the basis of these results, the 3/4-in inhibitor was chosen for further studies. Since some of the projectors used cones that were obtained from the Firestone Tire & Rubber Co. in which a cardboard "charge head" had provisions for a one-half inch diameter booster system, all subsequent projector studies were made using this booster diameter.

The effect of changing the head of composition B explosive extending above the spit-back tube was explored and the results are illustrated in figure 7 which shows radiographs of projectiles formed with explosive heads of (a) 1/4 in, (b) 3/4 in, and (c) 1-1/8 inches. Within the range of explosive heads tested the amount of projectile material is seen to increase as the column of explosive increases. Figure 7(a) indicates that a projectile is not formed when the short 1/4-in head of the explosive is used; figure 7(b) illustrates an acceptable projectile using an explosive head of 3/4 in, and figure 7(c) shows a long segmented projectile obtained when the explosive head is too high (1-1/8 inches).

From the foregoing tests, it is obvious that the formation of an acceptable projectile depends upon both the inhibitor height and column of explosive extending above the liner; the most successful half-scale arrangement was found employing a 3/4-in high inhibitor and a 3/4-in composition B explosive head.

Another set of radiographs are presented in figure 8 to demonstrate the reproducibility of projectile formation for a given design. Five projectiles obtained with charges having a 3/4-in inhibitor and a 3/4-in explosive head are shown. The projectile shown in figure 8(a) was from a Firestone machined cone and the

others are from cones machined in the Bureau shop at the Bruceton facility. Although certain differences exist in projectile detail and mass, the five radiographs show that this particular inhibitor-explosive arrangement gives reasonably reproducible results. Projectile velocities and estimates of the mass of the five projectiles are given in table 6. The measured projectile velocities vary from 9.1 km/sec to 9.4 km/sec and the masses (average 0.37 gram) are estimates based upon the apparent shape and size of the projectiles scaled from the photographs with the assumption that the projectile material has the normal density of aluminum.

A supply of 1/2-scale inhibited jet projectors, less explosive, was received from Firestone in which the cones had been formed by a rotary extrusion process and then machined to final dimensions. Performance trials with these projectors are now in progress.

The Scale II Air Cavity Projector

An air-cavity type projector was developed at the Ballistic Research Laboratories^{9/} that could propel a steel disk-shaped projectile having a mass of about 0.18 gram at a velocity of about 5 km/sec. The projector, designated as B.R.L. design #12, was used extensively in several hypervelocity impact programs. Recently, a version of this projector was tested whose linear dimensions were scaled upward by a factor of 2. If scaling laws hold, a projectile should be produced having the same velocity as the Scale I version with eight times the mass. This projectile would be useful because its kinetic energy would be comparable to

^{9/} Kineke, John H. Jr., and Lee S. Holloway. Macro-Pellet Projection with an Air-Cavity High Explosive Charge for Impact Studies. BRL Memorandum Report No. 1264, April 1960.

that of the 1/2-scale inhibited jet projectile and would provide a means for carrying out impact studies at constant energy as well as for allowing scaling studies to be made at about 5 km/sec.

A drawing of the scaled-up design is shown in figure 9. The projector consists of a 4-in diameter x 6-in long pentolite explosive charge with a 1-in diameter x 0.60-in air cavity at the base; the air cavity serves as a wave shaper. A 1-in diameter x 0.080-in thick steel disk is inserted in the lower portion of the air cavity. The initiation system consists of a 2-in diameter x 1-in long tetryl booster initiated by a short length of Primacord. The projectile that is produced is disk-shaped but comprises only a central portion of the original disk having about one-fifth of its initial mass.

Four of these projectors have been assembled and tested, three of which were used to impact "semi-infinite" lead targets to determine cratering characteristics and one was fired in the radiographic chamber for a projectile velocity measurement. The crater characteristics are useful in initial tests of this type because the appearance of the crater gives qualitative information regarding the integrity of the projectile at time of impact; if well-defined craters are formed, the crater volume is useful for estimating the projectile mass providing the velocity is known.

The craters for all four shots were well-formed and the crater measurements are given in table 7 and are compared with previous results^{10/} obtained from the B.R.L. #12 projector. On a scaled basis, the crater diameter, the crater depth, and crater

^{10/}Allison, F. E., K. R. Becker, and R. Vitali. Effects of Target Temperature on Hypervelocity Cratering. Fourth Symposium on Hypervelocity Impact, April 1960.

volume for the larger scale size are smaller than those from the B.R.L. design #12 by 4 percent, 6 percent, and 9 percent respectively. The differences may be due to the fact that the measured velocity of the scaled-up version is slightly less than 5.0 km/sec which is the velocity reported for the B.R.L. charge.

The velocity of the scaled projectile was determined from radiographs, one of which is shown in figure 10. The projectile is disk-shaped as expected and has a velocity of 4.7 km/sec.

An estimate of the projectile mass was obtained by assuming that crater volume per unit projectile energy is a constant. The assumption should be satisfactory since the crater volumes being compared here were made by projectiles having the same shape, the same composition, and about the same velocity. The value of the constant used is $2.64 \times 10^{-10} \text{ cm}^3/\text{erg}$ and was obtained by dividing the crater volume data given in table 7 (for the B.R.L. design #12) by the energy of that projectile. On this basis, a calculated mass of 1.46 grams was obtained that is within 1 percent of the expected scaled value.

The kinetic energy of the scaled projectile is therefore about $1.64 \times 10^{11} \text{ ergs}$ and this value compares favorably with the kinetic energy value possible with the 1/2-scale inhibited jet projector.

**TABLE 1. - Free surface distance-time results obtained
by pin technique using aluminum and brass
attenuators**

Tetryl Donor: 1 in diameter x 1 in long (density = 1.57)
Pin Spacing: .001, .011, .021, .031 in on a 1/2-in di-
ameter circle

Distance (in)	Time (μsec)	Average Time (μsec)
<u>1/4-in thick aluminum attenuator</u>		
0.001	0	0
0.011	0.161, 0.176, 0.145, 0.120, 0.166	0.154
0.021	0.322, 0.318, 0.290, 0.261, 0.289	0.296
0.031	0.483, 0.477, 0.452, 0.438, 0.456	0.461
<u>1/8-in thick brass attenuator</u>		
0.001	0	0
0.011	0.244, 0.234, 0.273, 0.238, 0.264	0.251
0.021	0.509, 0.520, 0.497, 0.533, 0.500	0.510
0.031	0.746, 0.738, 0.715, 0.800, 0.747	0.750

TABLE 2. - Wafer velocity and characteristic target damage for explosive-loaded aluminum targets designated Al-2024-T3

Shock Donor: 1-in diameter x 1-in long tetryl cylinder; density = 1.57 (gm/cm³)
 Wafer Dimensions: 1/2-in diameter x 1/32-in thick

Target Thickness (in)	Wafer Velocity (mm/ μ sec)	Pressure (kb)	Target Damage
1/8	2.13*	188	Circular perforation
	1.93*		do.
	2.03**		do.
	1.87**		do.
Average	<u>2.015</u>		
1/4	1.66	144	Circular perforation
	1.62		do.
	1.68		do.
	1.58		do.
	1.56		do.
	1.59		do.
Average	<u>1.612*</u>		
1/2	1.31	110	Circular perforation
	1.24		do.
Average	<u>1.275*</u>		
1.0	0.77*	63	Circular spallation
1-1/4	0.50*	39.2	Irregular spallation
1-3/8	0.44	33.0	Bulged and fractured
	0.42		do.
	0.42		do.
Average	<u>0.427*</u>		
1-1/2	0.36*	27.5	Bulged

* Average velocity over 13-cm path.

** Average velocity over 26-cm path.

**TABLE 3. - Wafer velocity and characteristic target
damage for explosive-loaded magnesium
targets designated AZ-31B-H24**

Target Thickness (in)	Wafer Velocity* (mm/ μ sec)	Pressure (kb)	Target Damage
3/32	3.28 3.58	189	Circular perforation do.
Average	<u>3.43</u>		
5/32	2.54 2.57	136	Circular perforation do.
Average	<u>2.555</u>		
3/8	1.90 1.94	95	Circular perforation do.
Average	<u>1.92</u>		
3/4	1.49	70	Irregular perforation and circular spallation
1.0	1.13	51	Irregular perforation and circular spallation
1-1/2	0.60	25	Circular spallation
2-3/4	0.47 0.45	19.5	Bulged and fractured do.
Average	<u>0.46</u>		

* Average velocity over 13-cm path.

TABLE 4. - Wafer velocity and characteristic target damage for explosive-loaded steel targets designated N-4130, S-18729,

BHT-54280

Shock Donor: 1-in diameter x 1-in long tetryl cylinder; density = 1.57 (gm/cm³)
 Wafer Dimensions: 1/2-in diameter x 1/32-in thick

Target Thickness (in)	Wafer Velocity (mm/ μ sec)	Pressure (kb)	Target Damage
1/8	1.01 1.03	214	Circular perforation do.
Average	<u>1.020</u>		
1/4	0.70 0.69	140	Irregular perforation and circular spallation
Average	<u>0.695</u>		
1/2	0.63 0.65	128	Circular spallation do.
Average	<u>0.64</u>		
5/8	0.61	120	Circular spallation
11/16	0.54 0.54 0.55	106	Irregular spallation do. do.
Average	<u>0.543</u>		
3/4	0.44	86	Bulged

TABLE 5. - Summary of spallation studies with
aluminum, magnesium, and steel
targets

Tetryl Donor - 1 in. diameter x 1 in. thick			
Target Material	Critical Thickness (in)	Critical Stress (kb)	
2024-T3 Aluminum	1-1/4 < t < 1-3/8	31	< p _s < 39
AZ-31B-H24 Magnesium	1-1/2 < t < 1-3/4	19.5	< p _s < 25
N-4130 Steel	11/16 < t < 3/4	86	< p _s < 106

TABLE 6. - Velocities and masses of scale 1/2
inhibited jet projectiles

Projectile Designation	Measured Velocity (km/sec)	Estimate of Mass (gm)
a	9.1	0.31
b	9.3	0.44
c	9.4	0.34
d	9.4	0.38
e	<u>9.1</u>	<u>0.38</u>
	$\bar{v} = 0.93$	$\bar{M} = 0.37$

**TABLE 7. - Comparison of crater dimensions in lead
targets for two scale sizes of air
cavity projectors**

	Scale II Version of B.R.L. Design #12	B.R.L. Design #12
Crater Depth	5.5 cm ($\sigma = 0.1$) ($n = 3$)	1/2 x 5.7 cm ($\sigma = 0.2$) ($n = 10$)
Crater Diameter	2.8 cm ($\sigma = 0.2$) ($n = 3$)	1/2 x 3.0 cm ($\sigma = 0.2$) ($n = 10$)
Crater Volume	43.4 cm ³ ($\sigma = 1.8$) ($n = 3$)	1/8 x 47.5 cm ³ ($\sigma = 1.5$) ($n = 10$)

Note: σ is the standard deviation per individual observation;
 n is the number of trials.

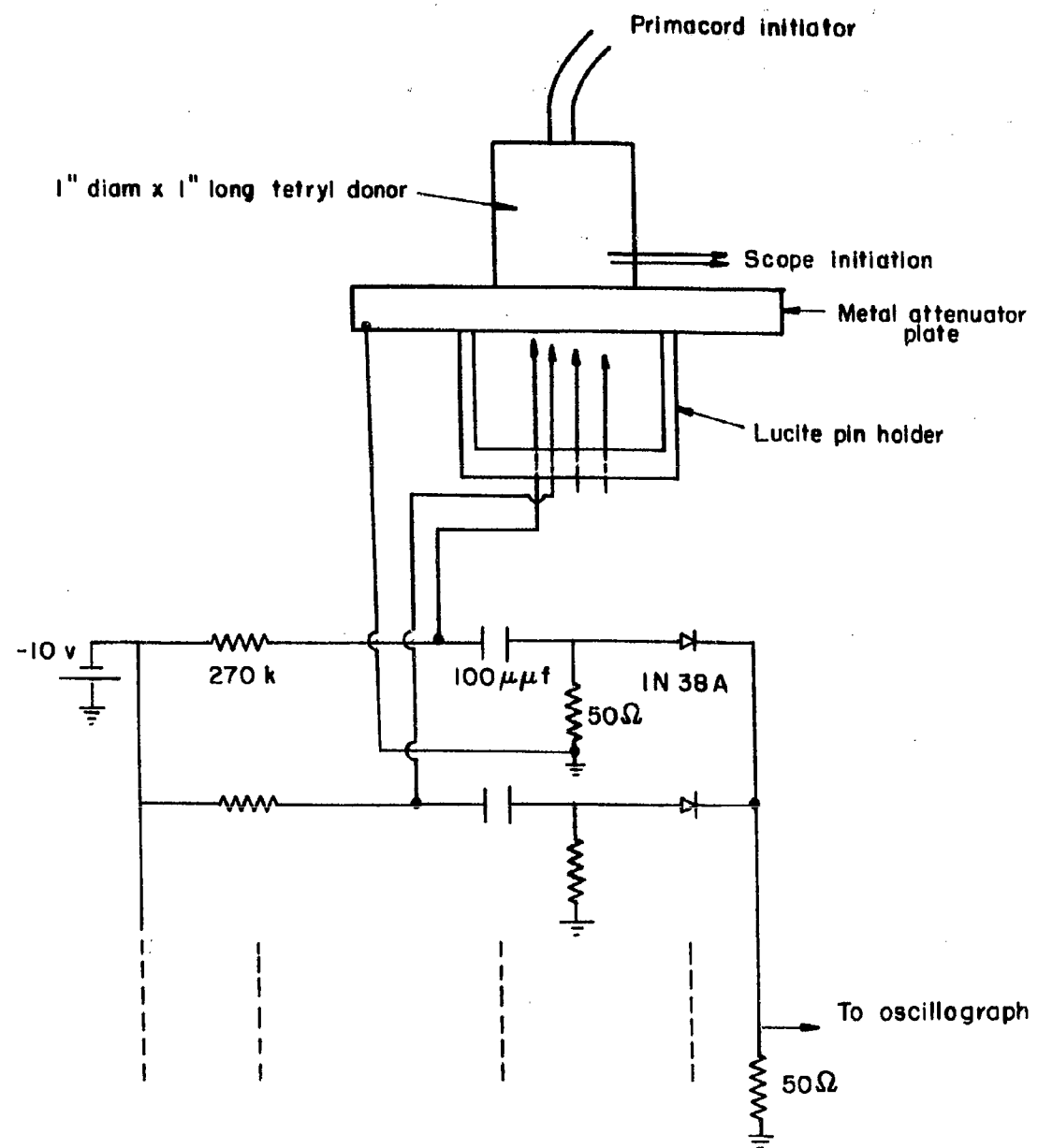


FIGURE 1. - Experimental arrangement used to determine free surface velocity of shocked metals.

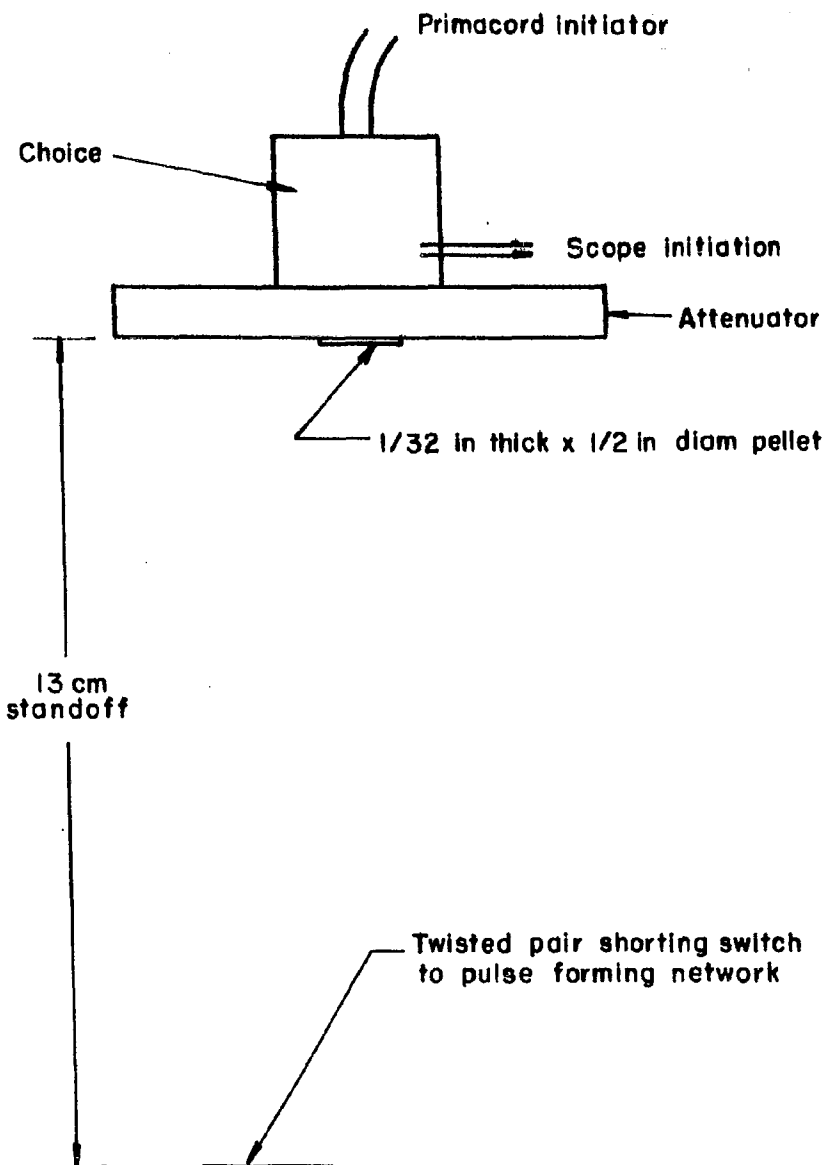
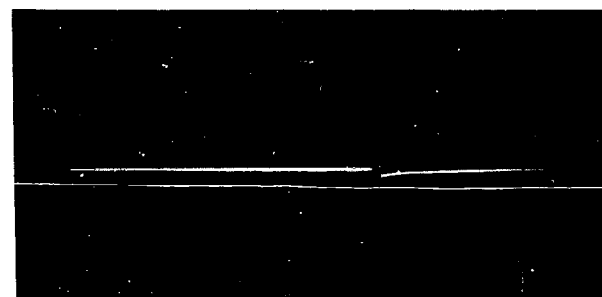


FIGURE 2. - Experimental arrangement used to determine average pellet velocity.



↔ 1.0 μ sec ↔

(a)



↔ 100 μ sec ↔

(b)

FIGURE 3. - Typical oscillogram obtained using
(a) the pin technique of figure 1,
and (b) the pellet experiment of
figure 2.

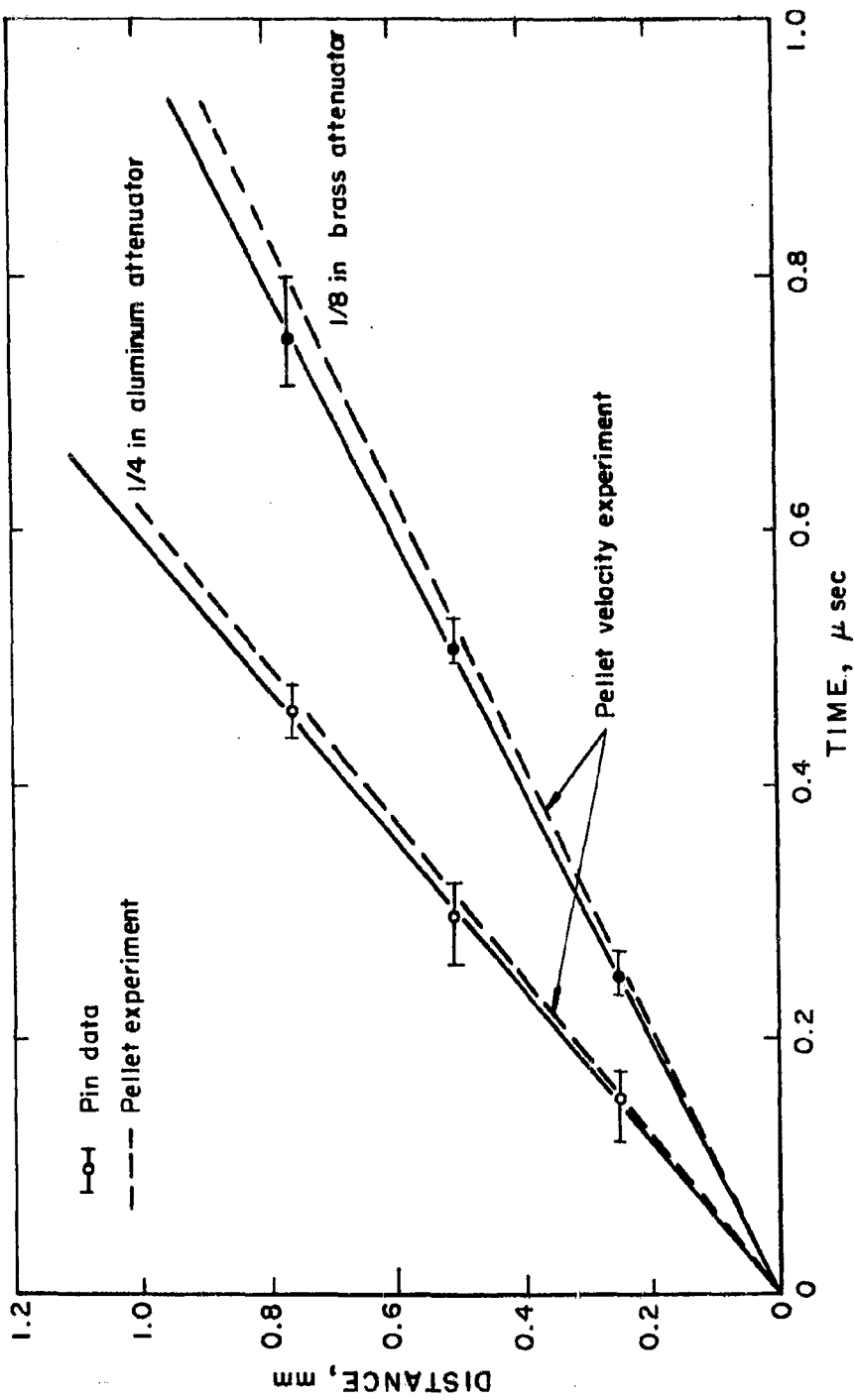


FIGURE 4. - A comparison of free surface velocity measurements obtained with two different techniques.

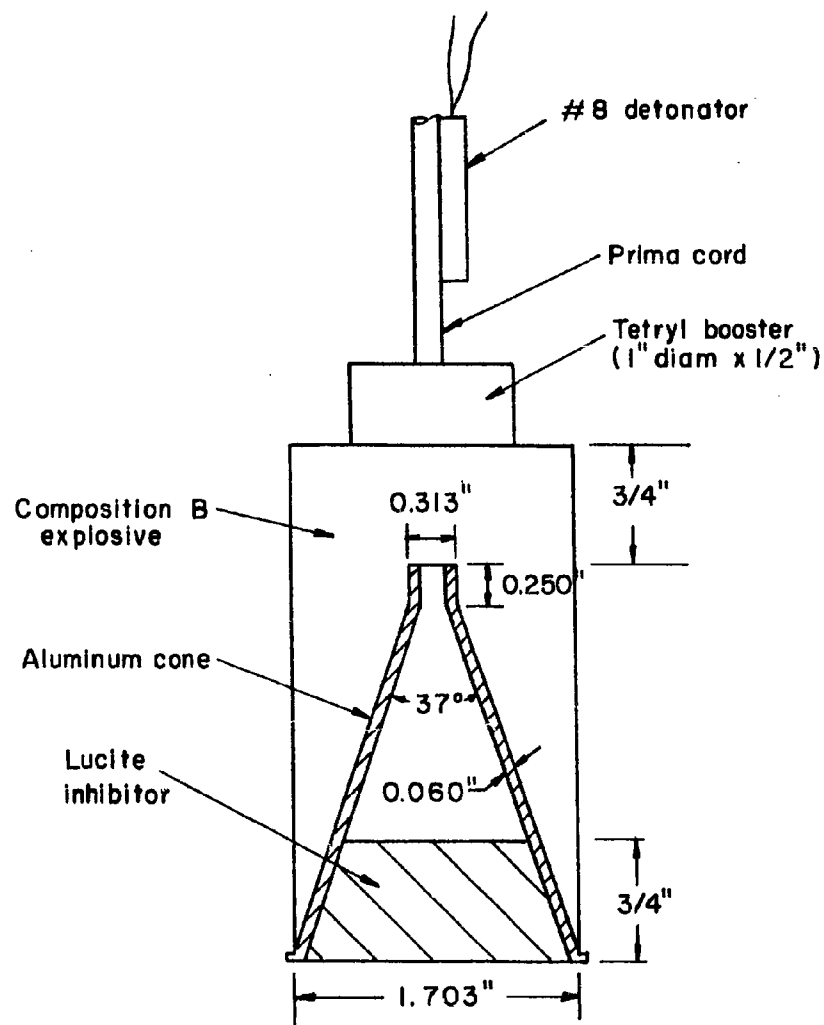


FIGURE 5. - Sketch of the essential features of the 1/2-scale inhibited jet projector.

(c)

(b)

(a)

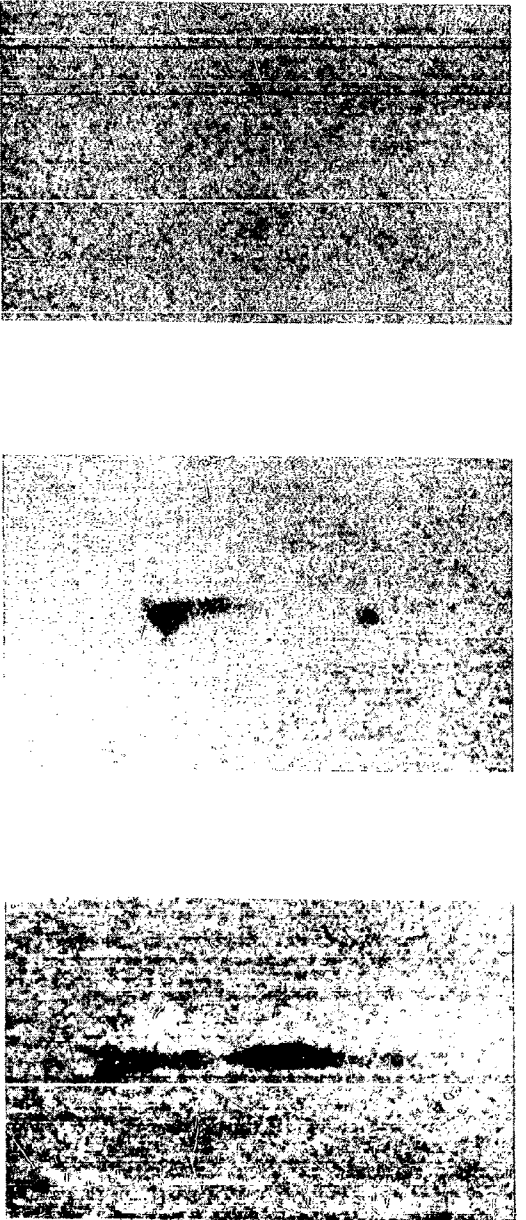


FIGURE 6. - Radiographs illustrating the effect that variations in inhibitor height have on projectile formation. Inhibitor heights are: (a) 5/8 in., (b) 3/4 in., and (c) 1 in.



FIGURE 7. - Radiographs illustrating the effect that variations in explosive column have on projectile formation. Explosive columns extending above split-tube are: (a) 1/4 in., (b) 3/4 in., and (c) 1-1/8 in.

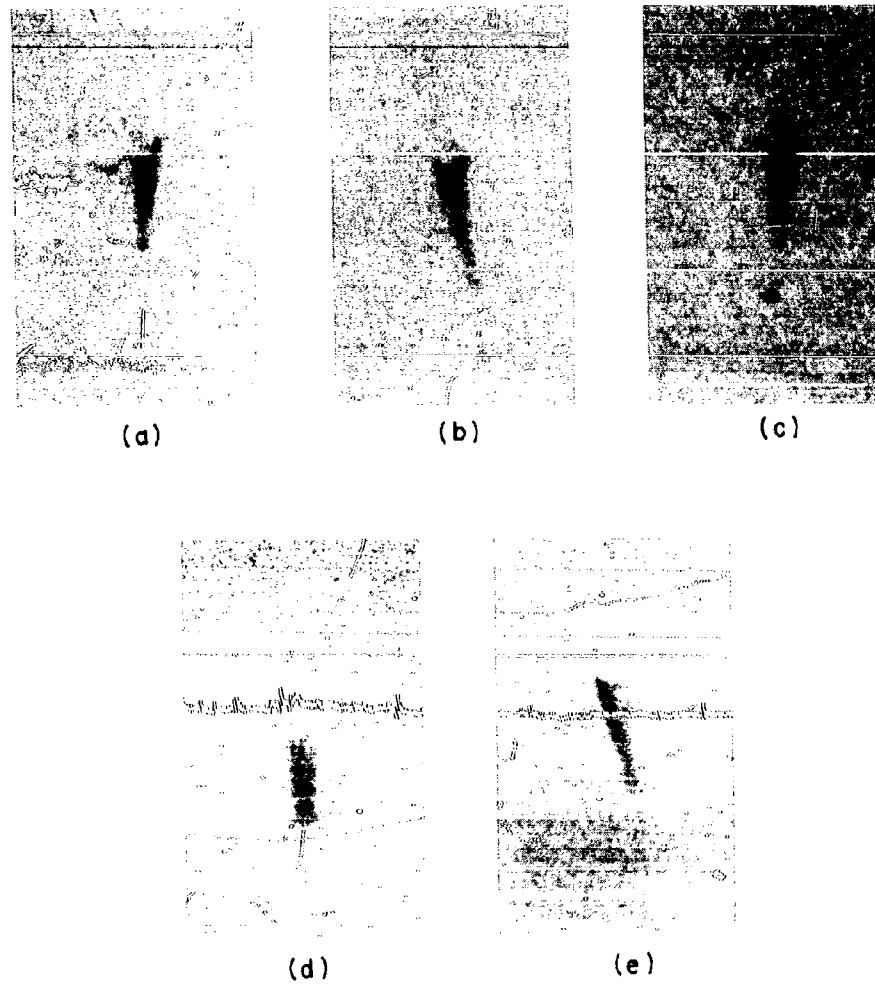


FIGURE 8. - Radiographs illustrating the degree of reproducibility obtained with projectiles formed by the 1/2-scale inhibited jet-type projector.

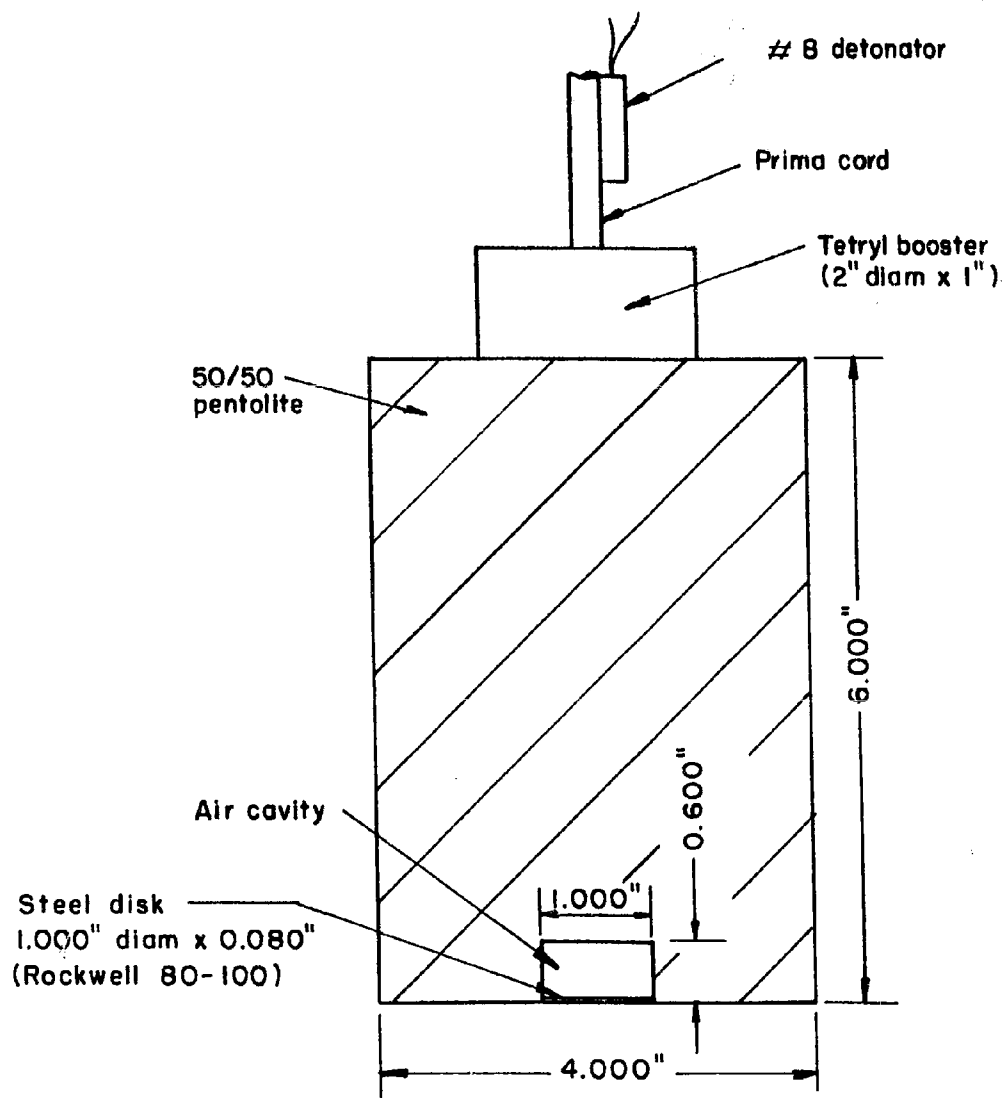


FIGURE 9. - Scale II version of B.R.L. Design #12,
air cavity projector.



FIGURE 10. - Radiograph of projectile produced by the scaled-up version of an air cavity projector.

**DISTRIBUTION LIST FOR
Type I Quarterly Report**

on

Hypervelocity Impact Phenomena

**Sponsored by the Department of the Army
Aberdeen Proving Ground**

**Commanding General
Aberdeen Proving Ground
Maryland
Attn: F. E. Allison
Ballistic Research Laboratories**

**Commanding General
Aberdeen Proving Ground
Maryland
Attn: S. Kronman
Ballistic Research Laboratories**

**Commanding General
Aberdeen Proving Ground
Maryland
Attn: R. J. Eichelberger
Ballistic Research Laboratories**

**Commanding General
Aberdeen Proving Ground
Maryland
Attn: J. Kineke
Ballistic Research Laboratories**

**Commanding General
Aberdeen Proving Ground
Maryland
Attn: Technical Library
Ballistic Research Laboratories**

**Office, Chief of Ordnance
Department of the Army
Washington 25, D. C.
Attn: ORDTU
Section
Mr. M. C. Miller**

**Office, Chief of Ordnance
Department of the Army
Washington 25, D. C.
Attn: ORDTU**

**Commanding Officer
Armed Services Technical
Information Agency
Arlington Hall Station
Arlington 12, Virginia
Attn: TIPCR**

**British Joint Services Mission
1800 K Street, N. W.
Washington 6, D. C.
Attn: Reports Officer**

**Canadian Army Staff
2450 Massachusetts Avenue
Washington 8, D. C.**

**Commanding Officer
U. S. Naval Ordnance Test Station
China Lake, California
Attn: J. W. Rogers**

**Director
U. S. Naval Research Laboratory
Washington 25, D. C.
Attn: Mr. W. W. Atkins, Code 130**

Commanding Officer
Air Proving Ground Center
Eglin Air Force Base, Florida
Attn: H. L. Davis

Detachment 4, ASD
(ASQWR, W. H. Dittrich)
Eglin Air Force Base
Florida

Director, The RAND Corporation
1700 Main Street
Santa Monica, California
Attn: J. H. Huth

Director, The RAND Corporation
1700 Main Street
Santa Monica, California
Attn: R. L. Bjork

Director, The RAND Corporation
1700 Main Street
Santa Monica, California
Attn: Technical Library

Library of Congress
Technical Information Division
Reference Department
Washington 25, D. C.
Attn: Bibliograph Section

General Motors Corporation
Defense Systems Div., Box T
Santa Barbara, California
Attn: J. W. Gehring

The Firestone Tire & Rubber Co.
1200 Firestone Parkway
Akron, Ohio
Attn: C. M. Cox

Commanding Officer
Air Proving Ground Center
Eglin Air Force Base, Florida
Attn: F. E. Howard
Det. 4, ASD(ASQP)

Director, National Aeronautics
& Space Administration
Ames Research Center
Moffett Field, California
Attn: Technical Library

Director, National Aeronautics
& Space Administration
Langley Research Center
Langley Field, Virginia
Attn: W. H. Kinard

Director, National Aeronautics
& Space Administration
Langley Research Center
Langley Field, Virginia
Attn: Technical Library

General Motors Corporation
Defense Systems Div., Box T
Santa Barbara, California
Attn: Technical Library

Aeroelastic & Structures
Laboratory
Massachusetts Institute of
Technology
77 Massachusetts Avenue
Cambridge 39, Massachusetts
Attn: W. Herrmann

Drexel Institute of Technology
Mechanical Engineering Dept.
Philadelphia 4, Pennsylvania
Attn: Pei Chi Chou

National Aeronautics & Space
Administration
Lewis Research Center
21000 Brookpark Road
Cleveland 35, Ohio

General Atomic Division
General Dynamics Corporation
P. O. Box 608
San Diego, California
Attn: J. M. Walsh

Director, National Aeronautics &
Space Administration
Ames Research Center
Moffett Field, California
Attn: J. L. Summers

Flight Physics Laboratory
Defense Research Laboratory, Box T
General Motors Corporation
Santa Barbara, California
Attn: A. B. Wenzel

Mr. A(be) Hake
The Martin Marietta Corp.
Baltimore 3, Maryland
Mail No. 3149

Headquarters S.S.D. (S.S.T.R.E.)
Air Force Unit Post Office
Los Angeles 45, California
Attn: Major Brewington

General Atomic Division
General Dynamics Corporation
P. O. Box 608
San Diego, California
Attn: M. F. Scharff

Pratt and Whitney Aircraft Div.
United Aircraft Corporation
East Hartford, Connecticut
Attn: H. Kraus

David Rich
General Electric Company
Missile & Space Division
Room U7225, Space Science Bldg.
Valley Forge, Pa.

Hughes Aircraft Company
Building 366, P. O. Box 90919
Los Angeles 9, California
Attn: I. G. Henry